A&A 477, 517–520 (2008)
DOI: 10.1051/0004-6361:20078781


Astronomy & Astrophysics

# Observations of the inner jet in NGC 1068 at 43 GHz

W. D. Cotton[1], W. Jaffe[2], G. Perrin[3], and J. Woillez[4]

[1] National Radio Astronomy Observatory⋆, 520 Edgemont Road, Charlottesville, VA 22903-2475, USA
e-mail: bcotton@nrao.edu
[2] Leiden Observatory, Neils BohrWeg 2, 2333 CA Leiden, The Netherlands
[3] Observatoire de Paris, LESIA, UMR 8109, 92190 Meudon, France
[4] W. M. Keck Observatory, 65-1120 Mamalahoa Highway, Kamuela, HI 96743, USA

Received 2 October 2007 / Accepted 6 November 2007

**ABSTRACT**

We present the results of observations of the AGN in the Seyfret galaxy NGC 1068 at 43 GHz (7 mm wavelength) with 50 mas resolution. The results are consistent with the claim of Gallimore et al. (2004) that the nuclear component is dominated by thermal emission. This adds to the growing body of evidence that this component is dominated by a hot inner region of the obscuring torus rather than the base of the radio jet. However, possible detection of linear polarization from this component suggests some emission from the synchrotron emitting jet or that the polarization arises from Thompson scattering of the thermal emission by the nuclear plasma.

**Key words.** Galaxy: nucleus – radio continuum: galaxies

## 1. Introduction

Active galactic nuclei (AGNs) exhibit strong emission all across the electromagnetic spectrum and can be studied even to great distance. AGNs show a diverse set of phenomena, many of which are thought to be determined by the angle at which the object is viewed. The "Unified" model of AGNs (Urry & Padovani 1995) is that the center of activity is a supermassive black hole being actively fed matter from an accretion disk. The release of gravitational potential heats the inner parts of the accretion disk to very high temperatures causing it to emit copious amounts of X-ray and UV radiation and very broad emission lines. Exterior to the accretion disk is thought to be an optically thick obscuring region of molecular gas and dust forming a disk-like "torus". Highly relativistic jets of plasma frequently occur along the poles of these systems which emit synchrotron emission which can be prominent at longer wavelengths. High energy radiation escaping along the poles of the torus ionize the ISM to distances of kpc resulting in strong, but narrow, emission lines.

The viewing angle has two effects. If the system is viewed pole on, shorter wavelength radiation escapes through the opening in the torus and the UV and broad emission lines are very easily visible. Emission from the highly relativistic jet, primarily radio and millimeter emission, is strongly amplified by Doppler boosting. Objects of this type are referred to as type 1 AGNs. If the system is viewed edge-on, the central region is obscured by the dust in the torus and the UV and broad emission lines are not seen. This is a type 2 AGN.

The AGN in the Seyfret 2 galaxy NGC 1068 has long been well studied at a number of wavebands (Muxlow et al. 1996; Gallimore et al. 1996b,a, 2004; Krips et al. 2006; Marco & Alloin 2000; Galliano & Alloin 2002; Galliano et al. 2005; Davies et al. 2006; Jaffe et al. 2004; Guainazzi et al. 2000). NGC 1068 is relatively nearby (14.4 Mpc, 1″ = 70 pc) so it can be studied with very good linear resolution. In the radio, an exhaustive study of NGC 1068 has been carried out by Gallimore et al. (1996b,a, 2004). The relativistic jet is prominent in radio emission and extends for several kpc in either direction. The jet undergoes an abrupt change of direction about 0.2″ from the nucleus in a region of bright radio and line emission. This change of direction is presumed to be the result of an interaction with a molecular cloud. Significant near- and mid-IR emission is associated with the inner radio jet (Marco & Alloin 2000; Jaffe et al. 2004; Galliano et al. 2005) which is presumed to the the result of shock heating of the dust in the ISM values by the passage of the jet. Long term variability in the IR is shown by Glass (2004) indicating variable output from the central engine. Further evidence for jet-ISM interaction is from Axon et al. (1997) who show that the ISM is in a higher ionization state near the radio jet.

The work of Gallimore et al. (1996b), Gallimore et al. (1996a) and Gallimore et al. (2004) establish their component S1 as the site of the central engine. This component has an inverted spectrum characteristic of optically thick synchrotron emission commonly seen in powerful AGN nuclei. However, they argue on the basis of observed brightness temperature, $10^5$ K too low to be opaque synchrotron, and morphology, the emission appears in a disk orthogonal to the direction of the jet, that this source is dominated by thermal emission from the inner portion of the torus. This is supported by the observations of $H_2O$ masers (Gallimore et al. 2001) nearly spatially coincident with the continuum emission. $H_2O$ masers are tracers of relatively dense, warm molecular gas. In contrast, Krips et al. (2006) interprete their results as showing a turnover in a synchrotron spectrum.

The high resolution mid-IR results of Jaffe et al. (2004) show large amounts of hot dust on similar size scales to the radio continuum which further supports the interpretation of this

⋆ The National Radio Astronomy Observatory (NRAO) is operated by Associated Universities Inc., under cooperative agreement with the National Science Foundation.

component as the inner region of the torus. The possible detection of linear polarization at 15 and 22 GHz by Gallimore et al. (1996b) has been interpreted as indicating that at least some of the emission has a synchrotron origin.

Recent work by Blundell & Kuncic (2007) on radio quiet quasars suggest that the radio emission from these objects in radio quiescent phases is dominated by optically thin thermal emission from an accretion disk wind rather than an opaque synchrotron source. These authors suggest that this may be a more general property of AGNs.

The bulk of the torus appears as a broad ring with a radius of several arc-seconds (~80 pc) as seen in $H_2$ emission (Galliano & Alloin 2002) and near-IR continuum (Marco & Alloin 2000). The lack of Br $\gamma$ emission suggests this material is shielded from the UV radiation field.

In the following, we present new VLA (Thompson et al. 1980) observations at 43 GHz at 50 mas resolution.

## 2. Observations and data reduction

The core of the galaxy NGC 1068 was observed using the VLA on 23 October 2000 at 43 GHz (a wavelength of 7 mm). The VLA was in A configuration with 21 antennas with the 43 GHz systems installed. However, the end antenna of the north arm did not have such a system and the next to the end antenna was broken; thus the length of the north arm was 12.3 rather than 18.9 km. The data were collected using two 50 MHz bands centered at 43.315 and 43.365 GHz in both right- and left-hand circular polarization. All combinations of polarizations were recorded.

The photometric calibration was based on the source J1331+305 (3C286) assuming a flux density of 1.45 Jy. Since J1331+305 is significantly resolved, only the inner three antennas on each arm were used to determine the flux density of the secondary photometric calibrator J0239-025 (0.70 Jy). Photometric calibration used 30 s vector averaging to reduce the effect of short term phase noise. The atmospheric opacity was measured in two tipping scans near the beginning and end of the observations; the two measurements were consistent at 0.08 nepers and this correction was used for all data. Corrections were also made using a standard gain curve for the VLA antennas.

Ten hours of observations were made in the "fast switching" mode with 70 s on NGC 1068 and 20 s on the astrometric and secondary photometric calibrator J0239-025. Antenna pointing corrections were determined and applied hourly. The weather was poor at the beginning of the observations but improved with time.

The instrumental polarization was determined from observations of J2202+422, J0238+166, J0319+415, J0242+110, and J0239-025. The polarization angle calibration was based on imaging of 1331+305 and using the sum of the Stokes $Q$ and $U$ CLEAN components. Similar treatment of J2202+422 gave reasonably consistent results.

After applying external calibration, the data on NGC 1068 were further adjusted using three iterations of phase self calibration. The final image includes 47.9 mJy of flux density. External calibration used the NRAO AIPS package (Greisen 1998) and self calibration and imaging used the Obit package (`http://www.cv.nrao.edu/~bcotton/Obit.html`).

Imaging used a weighting based on a Briggs robust parameter of 0 and a grid of pixels with a 10 mas spacing. This weighting is a good compromise between sensitivity and resolution.

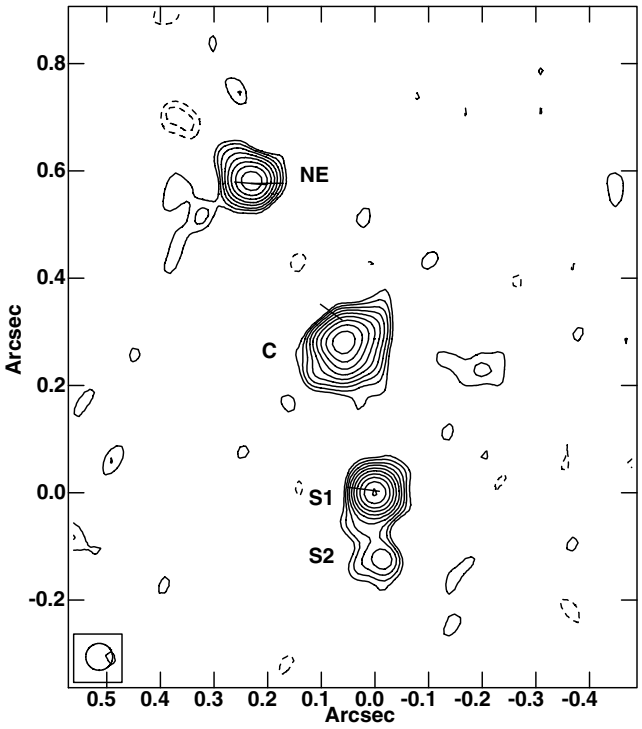


**Fig. 1.** Total intensity contours of NGC 1068 with superposed polarization E-vectors with lengths proportional to the bias corrected polarized flux density. Contours are at powers of $\sqrt{2}$ times 300 $\mu$Jy/beam; dashed contours are negative. Components are labeled with the nomenclature of Gallimore et al. (1996b). Positions are shown relative to the centroid of S1 which was determined by Gallimore et al. (1996b) to be the location of the core. The resolution is shown in the lower left corner.

The data were imaged and de-convolved using the CLEAN algorithm in Stokes $I$, $Q$ and $U$ (for a description of CLEAN see Cornwell et al. 1999). The CLEAN restoring beam was a circular Gaussian with *FWHM* of 50 mas.

## 3. Results

The derived image of NGC 1068 is shown in Fig. 1. In this figure and in the following discussion we will adopt the component nomenclature of Gallimore et al. (1996b). The off-source RMS noise in the Stokes $I$, $Q$ and $U$ images is 180 $\mu$Jy/beam.

At the resolution and surface brightness sensitivity of Fig. 1, only the regions of brightest emission are visible and none of the underlying jet shown by Gallimore et al. (1996b). Elliptical Gaussians were fitted to the components and these are given in Table 1.

### 3.1. Component spectra

The integrated flux densities from Table 1 for the identified components and various values from the literature are shown in Fig. 2. These data were made with a variety of resolutions and sensitivities resulting in a good deal of scatter in Fig. 2. Especially the VLBI results of Gallimore et al. (2004) (shown as plus signs) appear to have resolved out most of the flux density in most of these components. The 110 and 231 GHz data from Krips et al. (2006) were from low resolution data from which the extrapolated flux densities of components NE and C were removed. The flux densities presented here agree well with an

**Table 1.** Fitted elliptical Gaussian component parameters.

| Comp. | Integrated mJy | | Peak mJy | | Major mas | Axis | Minor mas | Axis | PA deg | |
|---|---|---|---|---|---|---|---|---|---|---|
| NE | 6.2 | (0.2) | 6.2 | (0.2) | <30 | | <30 | | | |
| C | 21.2 | (0.6) | 8.0 | (0.2) | 73.2 | (2.4) | 55.6 | (2.2) | 137 | (5) |
| S1 | 13.1 | (0.4) | 9.6 | (0.2) | 33.4 | (2.0) | 26.4 | (2.5) | 164 | (13) |
| S2 | 3.3 | (0.6) | 1.4 | (0.2) | 69.6 | (13.8) | 46.4 | (13.9) | 27 | (22) |

Formal 1 $\sigma$ errors given in parentheses.

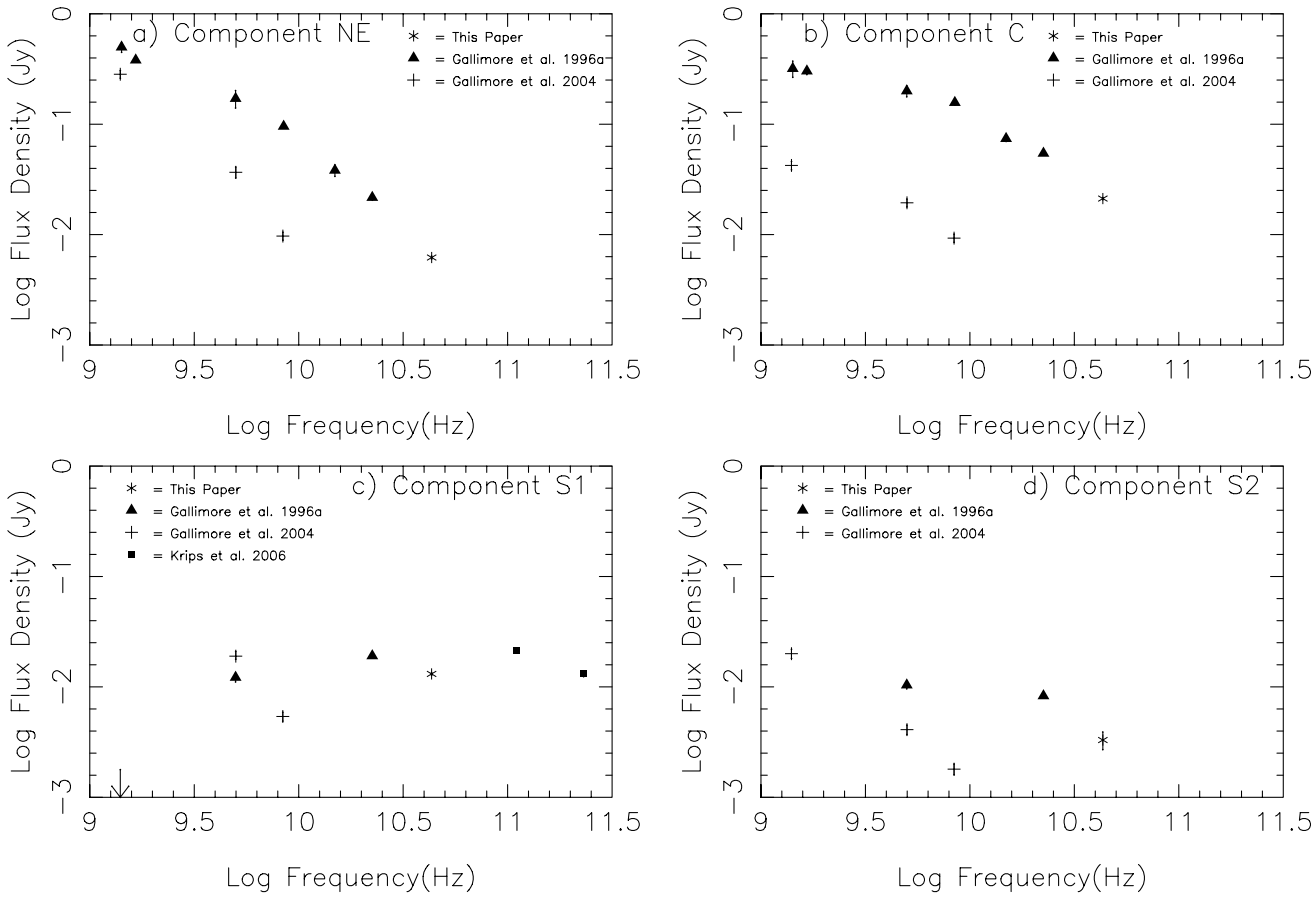


**Fig. 2.** Spectra of the components from data presented here and from the literature. Quoted error bars are plotted but are generally smaller than the symbols used.

extrapolation of the values for components NE and C found by Gallimore et al. (1996b).

Interpretation of the spectrum of the nuclear component shown in Fig. 2c is further complicated by the likelihood of variability. There is considerable scatter in this plot. Variation in the output of the central engine is seen in the variations of the $H_2O$ masers by Gallimore et al. (2001) and in the IR by Glass (2004).

### *3.2. Linear polarization*

The images of Stokes $Q$ and $U$ were converted to polarized intensity and polarization ("E") angle. The polarized amplitudes were corrected for bias using the standard methods and the polarized emission is shown in Fig. 1. This figure shows weak evidence for linear polarization in components S1 and NW. Gallimore et al. (1996b) also tentatively claimed the detection of linear polarization in these components.

The polarized signal at the peak of component S1 is 3.4 times the noise in $Q$ and $U$ and 6.2% of the total Stokes $I$. The orientation of the polarization vector is roughly perpendicular to the direction of the jet. If this is a real detection from optically thin synchrotron emission, then the magnetic field is oriented along the jet as is common in such sources.

The polarized signal at the peak of component NE is also 3.4 times the noise in $Q$ and $U$ and 10% of the total Stokes $I$. In this case, the polarization angle is roughly at 45° to the direction of the jet. In neither case is the detection of polarized emission beyond doubt, but the alignment of peaks in polarized emission with those is total intensity is encouraging.

If the polarization in Component S1 is real, an intriguing alternative to synchrotron emission is polarization of the thermal radiation by Thompson scattering as was suggested for X-ray polarization by Angel (1969). The dominant thermal emission indicates considerable plasma to do the scattering. This means of polarization depends on asymmetries in the source which is not implausible in this case. A further consideration is that if there is a dense circum-nuclear plasma, it is very likely that Faraday

depolarization will reduce any polarized emission coming from the nucleus.

## 4. Discussion

Gallimore et al. (1996b) identifies component S1 as the location of the central engine on the basis of its inverted/flat spectrum. However, this component is not predominantly the optically thick synchrotron source commonly seen in the nuclei of radio AGNs. Gallimore et al. (1996b) argues that the bulk of the emission is thermal in origin based largely on the low brightness temperature. In the data presented here, the brightness temperature is 8100 K which is more plausibly representative of thermal than optically thick synchrotron emission. However, this should be taken as a lower limit as any residual calibration errors will tend to broaden the component thereby reducing the derived brightness temperature.

The spectrum shown in Fig. 2c is consistent with a thermal source which is optically thick below 5 GHz (note upper limit at 1.4 GHz) and is relatively flat at higher frequencies. The claim of a dominant optically thick synchrotron source by Krips et al. (2006) appears not to be supported by Fig. 2c. The brightness temperature and spectrum of the nuclear component (S1) are in general agreement with the model of Blundell & Kuncic (2007) in which the nuclear emission is dominated by thermal emission from a hot wind from the accretion disk.

The higher resolution data from Gallimore et al. (2004) shows that the bulk of the emission comes from a linear feature roughly orthogonal to the direction of the jet and approximately co-spatial with $H_2O$ masers thought to inhabit the inner region of the torus. The fit to the data presented here given in Table 1 suggest a somewhat larger source whose principle elongation is along the jet; although, the significance of the orientation is unclear as the model fitted is nearly round. The difference with the results of Gallimore et al. (2004) at 8.4 GHz is likely due to the differences in resolution; Fig. 2c suggests that much of the flux density is resolved out at 8.4 GHz.

The high resolution mid-IR observations of Jaffe et al. (2004) show hot dust emission coincident with, and on a size scale comparable to, Component S1. This is also consistent with this being the inner region of the obscuring torus.

The possible detection of linear polarization both in the present work and by Gallimore et al. (2004) suggest that either not all of the emission is thermal or that the polarization is the result of Thompson scattering in the thermal plasma. The apparent polarization at 43 GHz of 6%, if real and due to synchrotron emission, would put an lower limit of 10% on the nonthermal fraction. Differential Faraday rotation in the circum-nuclear plasma is likely to reduce any linearly polarized emission.

The flux densities of the other components are consistent with an extrapolation of an optically thin synchrotron. At component C, the jet bends and line emission reported by Galliano & Alloin (2002) and Davies et al. (2006) as well as the presence of $H_2O$ masers, support the claim by Gallimore et al. (1996b) that the jet is diverted by interaction with a molecular cloud.

## 5. Conclusions

We present new 43 GHz 50 mas resolution images of the inner jet of NGC 1068. These results are consistent with the conclusion of Gallimore et al. (1996a) and Gallimore et al. (2004) and the model of Blundell & Kuncic (2007) that the emission from the nuclear component (S1) is dominated by thermal emission and does not confirm the suggestion by Krips et al. (2006) that the component is dominated by an optically thick synchrotron source. Thus, the evidence strongly points in the direction that Component S1 is dominated by thermal emission from the hot inner region of the obscuring torus rather than synchrotron emission from the base of the radio jet. However, the possible detection of linear polarization, both by us and Gallimore et al. (1996a) suggest either that 10% or more of the emission from S1 may be non-thermal synchrotron radiation, probably from the jet or, that the polarization comes from Thompson scattering from the plasma around the accretion disk. This latter possibility is also consistent with the model of Blundell & Kuncic (2007).

*Acknowledgements.* The authors would like to thank the anonymous referee for making suggestions leading to the improvement of this paper.

## References

Angel, J. R. P. 1969, ApJ, 158, 219
Axon, D. J., Marconi, A., Macchetto, F. D., Capetti, A., & Robinson, A. 1997, Ap&SS, 248, 69
Blundell, K. M., & Kuncic, Z. 2007, ApJ, 668, L103
Cornwell, T., Braun, R., & Briggs, D. S. 1999, in Synthesis Imaging in Radio Astronomy II, ed. G. B. Taylor, C. L. Carilli, & R. A. Perley, ASP Conf. Ser., 180, 151
Davies, R., Genzel, R., Tacconi, L., Mueller Sanchez, F., & Sternberg, A. 2006, ArXiv Astrophysics e-prints
Galliano, E., & Alloin, D. 2002, A&A, 393, 43
Galliano, E., Pantin, E., Alloin, D., & Lagage, P. O. 2005, MNRAS, 363, L1
Gallimore, J. F., Baum, S. A., & O'Dea, C. P. 1996a, ApJ, 464, 198
Gallimore, J. F., Baum, S. A., O'Dea, C. P., & Pedlar, A. 1996b, ApJ, 458, 136
Gallimore, J. F., Henkel, C., Baum, S. A., et al. 2001, ApJ, 556, 694
Gallimore, J. F., Baum, S. A., & O'Dea, C. P. 2004, ApJ, 613, 794
Glass, I. S. 2004, MNRAS, 350, 1049
Greisen, E. W. 1998, in Astronomical Data Analysis Software and Systems VII, ed. R. Albrecht, R. N. Hook, & H. A. Bushouse, ASP Conf. Ser., 145, 204
Guainazzi, M., Molendi, S., Vignati, P., Matt, G., & Iwasawa, K. 2000, New Astron., 5, 235
Jaffe, W., Meisenheimer, K., Röttgering, H. J. A., et al. 2004, Nature, 429, 47
Krips, M., Eckart, A., Neri, R., et al. 2006, A&A, 446, 113
Marco, O., & Alloin, D. 2000, A&A, 353, 465
Muxlow, T. W. B., Pedlar, A., Holloway, A. J., Gallimore, J. F., & Antonucci, R. R. J. 1996, MNRAS, 278, 854
Thompson, A. R., Clark, B. G., Wade, C. M., & Napier, P. J. 1980, ApJS, 44, 151
Urry, C. M., & Padovani, P. 1995, PASP, 107, 803